PROCEEDINGS OF SCIENCE

# Analysis of the Response of Silicon Photomultipliers to Optical Light Fields

**M. Ramilli**[*a], **M. Bondani**[bc], **A. Allevi**[c], **M. Caccia**[a], **A. Andreoni**[ac], **V. Chmill**[a]

[a] *Dipartimento di Fisica e Matematica, Università dell'Insubria, I-22100, Como, Italy*
[b] *National Laboratory for Ultrafast and Ultraintense Optical Science - CNR-INFM*
[c] *CNISM, U.d.R. Milano Università, I-20133 Milano, Italy*
*E-mail:* marco.ramilli@uninsubria.it, maria.bondani@uninsubria.it, alessia.allevi@uninsubria.it, massimo.caccia@uninsubria.it, andreoni@uninsubria.it, chmill@particle.kth.se

Silicon Photo-Multipliers (SiPMs) consist of a high density array of p-n junctions with a common output ($\sim 10^3$ cells per mm$^2$), operated beyond the breakdown voltage in a Geiger-Müller regime. With a typical gain of the order of $10^6$, time resolution at the 100 ps level, a dead time per diode limited to 100 ns, enhanced blue sensitivity, photon detection efficiency in excess of 30% and, notably, a photon number resolving capability up to a few tens of photons even at room temperatures, their performances are comparable with the common use Photo-Multiplier Tubes, with the advantage of operability in magnetic fields.

However, SiPMs present a significant Dark Count Rate (DCR), ranging from a few 100 kHZ to the MHz level at room temperature, and a relevant optical cross-talk between the cells, with values depending on the detector design and the biasing condition, so that their use is far from being trivial.

The performance of SiPMs have been tested in the context of the characterization of the photon number distribution in a light field. Infact, while the Geiger-Müller avalanche triggering by impinging photons can be modelized as a pure bernoullian process that preserves the photon number distribution of measured light field, relevant values of DCR and cross-talk can cause sizeable deviations from this statistics. Taking into account the DCR and cross-talk effects in the Geiger-Müller avalanche distribution, we demonstrate that photon number distributions in a poissonian and thermal-like light field can be properly reconstructed.

*9th International Conference on Large Scale Applications and Radiation Hardness of Semiconductor Detectors,RD09*
*September 30-October 2, 2009*
*Florence,Italy*

[*] Speaker.

 

PoS(RD09)030

| | Hamamatsu MPPC S10362-11-100C |
|---|---|
| Number of Diodes: | 100 |
| Area: | 1 mm $\times$ 1 mm |
| Diode dimension: | 100 $\mu$m $\times$ 100 $\mu$m |
| Breakdown Voltage: | **69.23** V |
| Dark Count Rate: | **540** kHz at 70 V |
| Optical Cross-Talk: | **25** % at 70 V |
| Gain: | $3.3 \cdot 10^6$ at 70 V |
| PDE (green): | 15 % at 70 V |

**Table 1:** Main characteristics of the SiPM (Hamamatsu, model MPPC S10362-11-100C). The data refer to room temperature.



## 1. Introduction

This paper focuses on SiPMs, detectors featuring unique characteristics that are achieved by a rapidly evolving technology [1, 2]. Silicon photomultipliers consist of a high density ($10^3$ mm$^2$) matrix of diodes with a common output. Each diode (or cell) is operated in a limited Geiger-Müller (GM) regime, in order to achieve gains at the level of $10^6$. Quenching mechanisms are implemented to avoid establishing self-sustaining discharges. These detectors are sensitive to single photons triggering GM avalanches and can be endowed with a dynamic range well above 100 photons/burst. The photon detection efficiency (PDE) depends on the sensor design and specification, but it may well exceed 30%. Moreover, SiPMs are genuine photon-number resolving detectors, measuring the light intensity simply by the number of fired diodes. Compactness, robustness, low cost, low operating voltage and power consumption are also added values against traditional photodetectors. On the other hand, SiPMs are affected by significant dark count rates (DCR hereafter), associated to cells fired by thermally generated charge carriers. Moreover, photon emission from the GM avalanches [3], may in turn trigger secondary avalanches and result in relevant optical cross-talk. While DCR and cross-talk may be directly measured, it is clear that they are folded in the detector response to any signal and need to be properly modelled if the statistical properties of the light have to be investigated (see ref. [4]). The self-consistent analysis of the statistics of light fields described in ref. [4] was performed using Hybrid Photo Detectors (HPDs) and Photo Multiplier Tubes (PMTs): testing its applicability using SiPMs as light detectors is one of the main motivations behind the study presented in this paper. However, this work features many similarities with a parallel and indipendent study described in ref. [5], with some differences that will be outlined in the text.

## 2. Experimental set-up

The experimental results reported below were obtained using SiPMs produced by Hamamatsu Photonics, namely model MPPC S10362-11-100C[1], whose main features are summarized in Ta-

[1] see http://www.hamamatsu.com

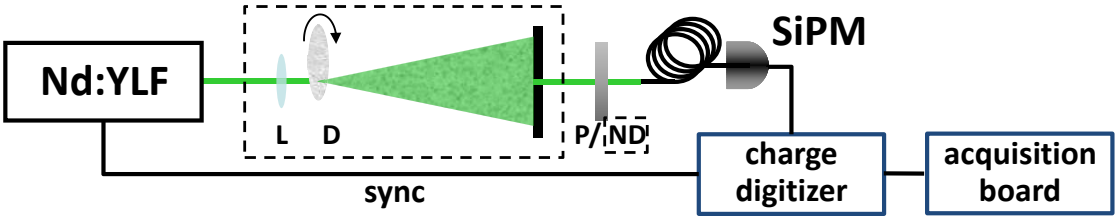


**Figure 1:** Experimental setup. Nd:YLF: laser source, P: polaroid, ND: variable neutral density filter, SiPM: detector. The components in the dashed boxes are inserted to produce the pseudo-thermal field.



ble 1. We illuminated the sensor with a frequency-doubled Nd:YLF mode-locked laser amplified at 500 Hz (High Q Laser Production) that provides linearly polarized pulses of $\sim$5.4 ps duration at 523 nm wavelength. We performed two series of measurements, the first one directly on the coherent laser output and the second one on the pseudo-thermal light obtained by passing the laser through a rotating ground-glass diffuser (D in Fig. 1) [6]. In order to vary the intensity of the delivered light, we inserted a rotating polarizer in the first serie of measurement, and a continuous variable neutral density filter in the second serie. We delivered the light to be measured to the sensor by a multimode optical fiber (1 mm core diameter).
The signal was integrated by a charge digitizer V792 produced by CAEN[2], with a 12-bit resolution over 400 pC range; the signal was typically integrated over a 200 ns long time window synchronized to the laser pulse.

## 3. The Model

The response of an ideal detector to a light field can be described in a simple way as a bernoullian process:

$$B_{m,n}(\eta) = \binom{n}{m} \eta^m (1-\eta)^{n-m} \,. \tag{3.1}$$

where $B_{m,n}(\eta)$ is the bernoullian probability of having $m$ events out of $n$ trials, each event having a probability of occurrence $\eta$: in our case, $n$ is the number of impinging photons over the integration time, $m$ the number of detected photons and $\eta < 1$ the photon-detection efficiency. Actually, $\eta$ is a single parameter quantifying detector effects and losses (intentional or accidental) which can be tracked to the optical system. As far as SiPMs are concerned, detector effects are due to the quantum efficiency, the fill factor and the avalanche triggering probability, namely the probability for a charge carrier to develop a Geiger-Müller quenched discharge [7, 8]. As a consequence, the distribution $P_{m,\mathrm{el}}$ of the number of the GM avalanches triggered by a photo-electron actually corresponding to a detected photon, must be linked to the distribution $P_{n,\mathrm{ph}}$ of the number of photons

[2] http://www.caen.it

in the light beam under measurement by

$$P_{m,\mathrm{el}} = \sum_{n=m}^{\infty} B_{m,n}(\eta) P_{n,\mathrm{ph}} \ . \tag{3.2}$$

This simple description has to be further developed to link $P_{m,\mathrm{el}}$ to the probability density distribution of the GM avalanches of any origin. First we must take into account spurious hits and cross-talk effects, not negligible in the detectors being studied. As in our experimental setup the acquisition is performed by signal current integration and not by waveform digitalization (as instead done in ref. [5]), we cannot reject the contribution of dark count events occurring in the gate of integration; we thus decided to model their contribution as a a poissonian process which can be described as:

$$P_{m,\mathrm{dc}} = \frac{\overline{m}_{\mathrm{dc}}^{m}}{m!} e^{-\overline{m}_{\mathrm{dc}}}, \tag{3.3}$$

where $\overline{m}_{\mathrm{dc}}$ is the mean number of dark counts observed in the integration time.

As a consequence, the statistics of the recorded pulses may be described as:

$$P_{m,\mathrm{el+dc}} = \sum_{i=0}^{m} P_{i,\mathrm{dc}} P_{m-i,\mathrm{el}}. \tag{3.4}$$

As a further step, cross-talk effects shall be taken into account. Cross-talk is a genuine cascade phenomenon that can be described at first order as [5]

$$C_{m,n}(\varepsilon) = \begin{pmatrix} n \\ m-n \end{pmatrix} \varepsilon^{m-n} (1-\varepsilon)^{2n-m} \ , \tag{3.5}$$

being $\varepsilon$ the (constant) probability that the GM avalanche of a cell triggers a second cell, $n$ the number of dark counts and photo-triggered avalanches and $m$ the total number of detected GM avalanches. Within this first-order approximation, the actual sensor response is described by

$$P_{m,\mathrm{cross}} = \sum_{n=0}^{m} C_{m,n}(\varepsilon) P_{n,\mathrm{el+dc}} \ . \tag{3.6}$$

In actual data analysis, further steps of the cascade had been added, adding terms like equation 3.5, each one providing additional $m-n$ events out of $n$ events triggered in the previous step of the cascade.

## 4. Data Analysis

### 4.1 Procedure Overlook

Recorded spectra were analyzed in a two-step procedure:

- we measured the area of each spectrum peak, corresponding to the spread of the signal around its mean value (given by the peak position) due to stocastic terms: thus the area $A_m$ of the $m$-th peak is a measurement of $P_{m,\mathrm{cross}}$ ;

- we fitted the obtained data points with a theoretical function, which takes into account the statistics of light, detection and all deviations of the detectors from ideality, such as DCR and cross-talk effects, as shown in section 3.

To evaluate the area of each peak, we performed a multi-peak fit of the spectrum histogram, modelling each peak with a Gauss-Hermite function (GH) [9]:

$$\mathrm{GH} \;=\; Ne^{-w^2/2}\left[1+{}^3hH_3(w)+{}^4hH_4(w)\right], \tag{4.1}$$

where

$$w \;=\; \frac{x-\bar{x}}{\sigma} \tag{4.2}$$

and $N$ is a normalization factor, $\bar{x}$ is the peak position and $\sigma$ is the variance of the gaussian function; $H_3(w)$ and $H_4(w)$ are the third and the fourth normalized hermite polynomials, giving respectively a completely asymmetric and a completely symmetric deviation from the gaussian shape. These deviations are used to take into account the phenomenological asymmetry of the peaks. The deviation from gaussian shape is regulated by the pre-factors ${}^3h$ and ${}^4h$, with values in the range $[-1,1]$. The global fit function of the spectrum is a sum of as many Gauss-Hermite function as the number of resolved peaks.
The choice of the GH-function in Eq. (4.1) allows us to calculate the area $A_m$ in a very straightfoward way, simply by the relation

$$A_m \;=\; N_m\,\sigma_m\,(\sqrt{2\pi}+{}^4h_m); \tag{4.3}$$

The error $\sigma_{A_m}$ on the obtained value is calculated by propagating the errors on the fit parameters; these values are then used to fit the final Geiger-Müller avalanches probablity distribution $P_{m,\mathrm{cross}}$ (see equation 3.6).
The main limit of this approach is obvious: as all the information on the statistics of the system is obtained from the peak areas, this method can only be applied to peak-resolving histograms with a number of peaks greater than the number of free parameters of the fitting function, which, in the present analysis, can rise up to five.

### 4.2 Poissonian Light

We measured the statistics of 20000 subsequent laser shots in 15 series, each one with a different mean value set by rotating a polarizer (P in Fig. 1) in front of the collection fiber.
Being in this case $P_{m,\mathrm{el}}$ of equation 3.2 a poissonian distribution, we have a theoretical fitting funtion with three free parameters: the expectation value of the number of avalanches generated by the light field and DCR ($\overline{m}_{\mathrm{el+dc}}$), the probability $\varepsilon$ for an avalanche to trigger a second one and a global normalization factor: in this case we are limited to spectra with at least 4 resolved peaks.

In Figure 2(a) we show an example of the results obtained with the multi-peak fit procedure on a spectrum obtained from poissonian light, while in Figure 2(b) we show the obtained data points representing the statistics of the Geiger-Müller avalanches, fitted both with a simple poissonian distribution and with our probability distibution taking into account cross-talk effects: using the $\chi^2$ as an indicator of the goodness of the result, our model proves to provide an excellent description of the phenomena.

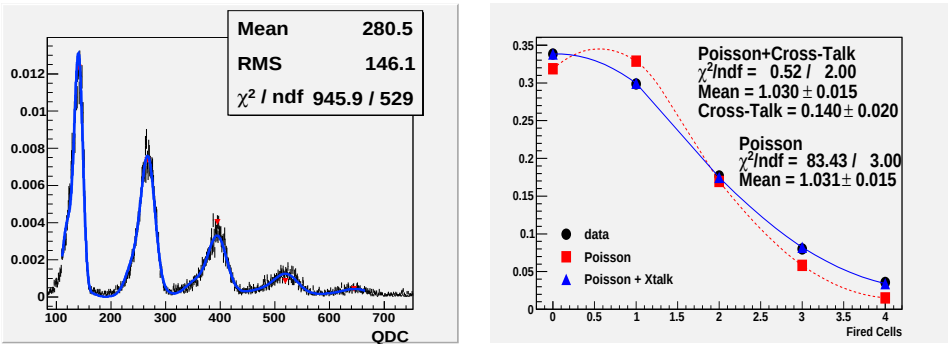


(a) (b)

**Figure 2:** (a) result of the multi-peak fit procedure on a spectrum obtained with poissonian light; (b) fit of the peak areas $A_m$ (full points) with the theoretical function (eq. 3.6) including cross-talk contribution (triangles, solid line), compared with a fit with a poissonian distribution (squares, dashed line). The lines are only to guide the eye through the experimental and fitted points.

### 4.3 Single Mode Pseudo-Thermal Light

In order to obtain information on the contribution of dark-counts we measured a different light statistics, with a shape modified by the convolution with the poissonian distribution for dark-counts. We measured a single mode pseudo-thermal light distribution, with an expected probability distribution function of

$$P_{m,\mathrm{el}} = \overline{m}_{\mathrm{el}}^{m} / (\overline{m}_{\mathrm{el}} + 1)^{m+1}. \tag{4.4}$$

We produced the above mentioned light field by selecting with a small aperture ($\sim 150\ \mu$m diameter) a region much smaller than the coherence area of the speckle patterns produced by the rotating diffuser. We follow the same procedure described for coherent light by measuring the values of the output at 50000 subsequent laser shots and at 10 different mean values, obtained by means of a variable neutral-density filter (ND in Fig. 1).

Like in previous subsection, we show in Figure 3 an example of the results obtained from our analysis of the spectra. In Figure 3(a) we present the multi-peak fit of a typical spectra corresponding to the output of a sensor illuminated with a single mode pseudo-thermal light field; in Figure 3(b), we compare our fitted probability distribution, with the one without DCR and cross-talk contributions: again, $\chi^2$ is an indication of the goodness of our model.

## 5. Conclusions

The experimental tests we performed proved that our model provides a realistic descritption of the response of a Silicon Photomultiplier, allowing us to take into account the deviations to the statistics of light induced by the non-idealities of the sensor.
This method of analysis, together with direct measurements of DCR and optical cross-talk, can prove particulary useful when statistic of light has to be reconstructed precisely; an example of

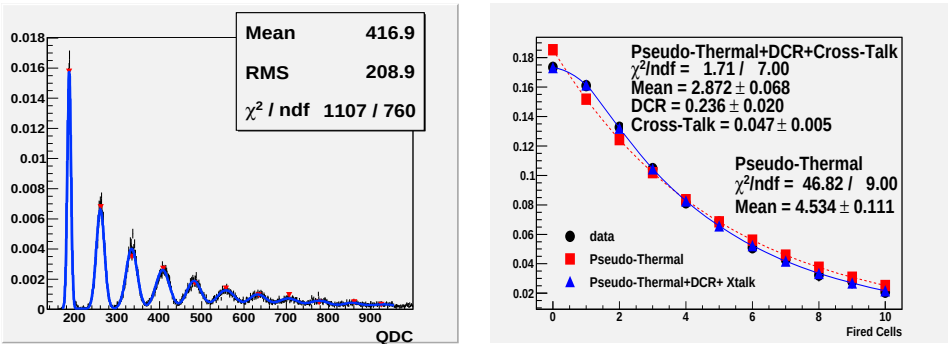


(a) (b)

**Figure 3:** (a) result of the multi-peak fit procedure on a spectrum obtained with single mode pesudo-therml light; (b) fit of the peak areas $A_m$ (full points) with the theoretical function (eq. 3.6) including dark count rate and cross-talk contribution (triangles, solid line), compared with a fit with a single mode pseudo-thermal (squares, dashed line). The lines are only to guide the eye through the experimental and fitted points.

a possible application consists in the use of SiPMs in Fluorescence Fluctuations Spectroscopy (FFS) techniques, particularly in Photon Counting Histogram (PCH) [10, 11], where parameters of biophysical interest (such as the mean number of emitting particles) are obtained from the deviation from poissonian distribution of fluorescence light emission: in this situation, a precise knowledge of other sources of deviation is of utmost importance.

## References

[1] B. Dolgoshein et al., "Status report on silicon photomultiplier development and its applications," Nucl. Instrum. Methods Phys. Res. A **563**, 368-376 (2006).

[2] J. Haba, "Status and perspectives of Pixelated Photon Detector (PPD)," Nucl. Instrum. Methods Phys. Res. A **595**, 154-160 (2008).

[3] F. Zappa, S. Cova, M. Ghioni, A. Lacaita, C. Samori, "Avalanche photodiodes and quenching circuits for single-photon detection," Appl. Opt. **35**, 1956-1976 (1996).

[4] M. Bondani, A. Allevi, A. Agliati, and A. Andreoni, "Self-consistent characterization of light statistics," J. Mod. Opt. **56**, 226-231 (2009).

[5] I. Afek, A. Natan, O. Ambar, and Y. Silberberg, "Quantum state measurements using multipixel photon detectors," Phys. Rev. A **79**, 043830(1-6) (2009).

[6] F. T. Arecchi, "Measurement of the Statistical Distribution of Gaussian and Laser Sources," Phys. Rev. Lett. **15**, 912-916 (1965).

[7] K. G. McKay, "Avalanche Breakdown in Silicon," Phys. Rev. **94**, 877-884 (1954).

[8] W. G. Oldham, R. R. Samuelson, P. Antognetti, "Triggering phenomena in avalanche diodes," IEEE Trans. Electron. Dev. **ED-19**, 1056-1060 (1972).

[9] R. P. Van Der Marel and M. Franx, "A new method for the identification of non-gaussian line profiles in elliptical galaxies," ApJ **407**, 525-539 (1993).

[10] Y. Chen, J.D. Müller, P.T.C. So and E. Gratton, “The Photon Counting Histogram in Fluorescence Fluctuation Spectroscopy”, Biophys. J. **77**, 553-576 (1999)

[11] L.N. Hillesheim and J.D. Müller “The Dual-Color Photon Counting Histogram with Non-Ideal Photodetectors”, Biophys. J. **89**, 3491-3507 (2005)